Hybrid Geometric Optical–Radiative Transfer Model Suitable for Forests on Slopes

Weiliang Fan, Jing M. Chen, Weimin Ju, and Nadine Nesbitt

***Abstract*—A new geometric optical (GO)–radiative transfer (RT) model with a multiple scattering scheme suitable for sloping forest canopies is developed in this study. It is based on a Geometrical–Optical model for Sloping Terrains and an RT method. This new model overcomes the difficulty to prescribe bidirectional reflectance factors (BRFs) of shaded components (shaded foliage and background) in GO modeling through simulating radiation multiple scattering within a sloping forest. A case study shows that multiply scattered radiation depends on topographic factors and leaf area index. The contributions of the shaded components to stand-level BRF are less than 3% in the red band and can reach up to 40% in the near-infrared (NIR) band. The "multiangle" Moderate Resolution Imaging Spectroradiometer (MODIS) data over sloping pixels are selected to validate the modeled forest BRF. Considering the multiple scattering schemes and topographic factors, the modeled BRF is closer to the MODIS surface reflectance (BRF product) (red band: $R^2 = 0.8614$, rRMSE $= 0.1339$; NIR band: $R^2 = 0.7573$, rRMSE $= 0.0850$) than the modeled BRF (red band: $R^2 = 0.7771$, rRMSE $= 0.1839$; NIR band: $R^2 = 0.5176$, rRMSE $= 0.1155$) without topographic consideration. It is also shown that the MODIS surface reflectance of sloping forests at multiple angles can be simulated well using the newly developed model.**

***Index Terms*—Forest reflectance model, forests on slopes, geometric optical (GO) model, multiple scattering, radiative transfer (RT) model.**

I. Introduction

The reflected radiation from a forest is determined by complex canopy structure and scattering behavior of the foliage. For understanding remote sensing measurement of reflected radiance above forests, many forest reflectance models have been developed [1]–[4]. The geometric optical (GO) modeling approach, which separates a forest into four scene components (sunlit foliage, shaded foliage, sunlit background, and shaded background), is an efficient and useful way to simulate bidirectional reflectance factor (BRF) of forest stands by considering the geometry of canopy structures, such as tree crowns and branches. However, previous GO models have only considered trees growing on horizontal surfaces [1], [2] rather than sloping surfaces. Many studies indicate that forest BRF is significantly influenced by topographic factors [5]–[7]. For a more accurate simulation of sloping forest BRF, a Geometrical–Optical model for Sloping Terrains (GOST) has been developed [8] based on the four-scale GO model [2]. In GOST, the mathematical description for the projection of tree crowns on the ground has been modified to consider the fact that trees grow vertically rather than perpendicular to sloping grounds. The same as the four-scale GO model, the GOST model can also simulate the shape of trees as cone, ellipsoid or "cone + cylinder." A simplified ray-tracing procedure has also been employed to separate the sunlit and shaded foliage. A case study shows that differences in forest component area ratios between flat and sloping terrains can reach up to 50%–60% in the principal plane and about 30% in the perpendicular plane [8].

In forests growing on flat surfaces, radiative multiple scattering within the canopy and soil system has a strong impact on canopy BRF [9], and we would expect that the scattering processes are greatly modified for forests on sloping terrains. Further exploration of the relationship between forest BRF and remote sensing observations should consider a multiple scattering scheme suitable for sloping canopies. However, no such GO models have so far been developed. Generally, there are three kinds of forest reflectance models for simulating the multiple scattering within flat forests, i.e., view factors, ray tracing, and radiative transfer (RT) methods. Chen and Leblanc use view factors among forest scene components and the sky [9]. Due to the mathematical complexity in describing these view factors, many simplifications are made in view factor calculations, leading to considerable uncertainties in the simulated BRF. Ray tracing is theoretically an ideal way to simulate the complex multiple scattering process [10], but it is practically limited by computing resources and its accuracy would depend on the amount of structural detail included in the preset scene [4]. RT methods are suitable for considering multiple scattering within turbid media rather than canopies with organized structures [11], [12]. Recognizing the different advantages of the GO and RT models, several researchers introduced RT procedures into GO models to simulate multiple scattering within a flat canopy [4], [13]. These models demonstrate a good combination between GO and RT models. On the other hand, the contributions of the shaded components to the total forest

Manuscript received May 6, 2013; revised July 28, 2013; accepted November 7, 2013. Date of publication January 16, 2014; date of current version May 1, 2014. This work was supported in part by the National Science Foundation of China under Grant 41271352/D0106, by the National Basic Research Program of China under Grant 2010CB950704, and by the Chinese Academy of Sciences for Strategic Priority Research Program under Grant XDA05050602.

W. Fan and W. Ju are with the International Institute for Earth System Science and the Jiangsu Provincial Key Laboratory of Geographic Information Science and Technology, Nanjing University, Nanjing 210046, China (e-mail: fanweiliang@163.com; juweimin@nju.edu.cn).

J. M. Chen is with the International Institute for Earth System Science and the Jiangsu Provincial Key Laboratory of Geographic Information Science and Technology, Nanjing University, Nanjing 210046, China, and also with the Department of Geography and Program in Planning, University of Toronto, Toronto, ON M5S 3G3, Canada (e-mail: jing.chen@utoronto.ca).

N. Nesbitt is with the Department of Geography and Program in Planning, University of Toronto, Toronto, ON M5S 3G3, Canada (e-mail: nadine.nesbitt@utoronto.ca).

Digital Object Identifier 10.1109/TGRS.2013.2290590

BRF are very difficult to measure *in situ* or to quantify using GO models [14], [15]. Several models treat these components as negligible and/or having no spectral dependence [16], while it is generally known that multiple scattering is particularly strong in the near-infrared (NIR) band in which leaf scattering albedo is close to unity [17]. In order to estimate the BRF of the shaded components, it is therefore necessary to have a reasonably accurate multiple scattering scheme in a GO model.

In this paper, the GOST model and an RT model are combined to develop a new forest reflectance model, which considers both multiple scattering and topographic factors within a canopy. The objectives of this study are as follows: 1) to parameterize the BRFs of the shaded components of sloping forests using architectural parameters and the scattering behavior of forest components and 2) to simulate and validate the BRF of sloping forests using satellite data.

II. Theory

Forest BRF is generally treated as the weighted average of the four components

$$\mathrm{BRF}(\lambda) = r_T(\lambda)\cdot P_T + r_G(\lambda)\cdot P_G + r_{ZT}(\lambda) \cdot P_{ZT} + r_{ZG}(\lambda)\cdot P_{ZG} \tag{1}$$

where r_T, r_G, r_{ZT}, and r_{ZG} are BRF values of the sunlit foliage, sunlit background, shaded foliage, and shaded background, respectively, which include multiply scattered radiation within a sloping forest. The sunlit foliage and background can be reached by the direct and diffuse solar radiation, and the shaded foliage and background can only be reached by diffuse radiation. P_T, P_G, P_{ZT}, and P_{ZG} are the area ratios of the sunlit foliage, sunlit background, shaded foliage, and shaded background in a particular view direction, respectively, which are wavelength independent.

A. Area Ratios of the Four Components on Sloping Forests

The GOST model has been developed for simulating area ratios of the four scene components on sloping forests based on the four-scale GO model [8]. In GOST, the gap fraction theory is used for separating the foliage $(1 - Pvg)$ and background (Pvg) first. Second, the sunlit background (P_G) and shaded background (P_{ZG}) are separated using a "hot-spot function" (2), and finally, the sunlit foliage (P_T) and shaded foliage (P_{ZT}) are separated using a simplified ray-tracing model (3)

$$P_{ZG} = Pvg - P_G \tag{2}$$
$$P_{ZT} = 1 - Pvg - P_T. \tag{3}$$

B. BRFs on Sloping Forests

The BRF of the four scene components are

$$r_{ZT}(\lambda) = S_{bs}(\lambda) \tag{4}$$
$$r_{ZG}(\lambda) = S_{sc}(\lambda) \tag{5}$$
$$r_T(\lambda) = R_T + S_{bs}(\lambda) \tag{6}$$
$$r_G(\lambda) = R_G + S_{sc}(\lambda) \tag{7}$$

where R_T and R_G are the first-order BRFs of the foliage and background, respectively. $S_{bs}(\lambda)$ and $S_{sc}(\lambda)$ are the multiply scattered BRFs of the shaded foliage and background, respectively. The BRF of sunlit components is also enhanced by the same amounts attributed to multiple scattering.

1) BRF of Shaded Background $S_{sc}(\lambda)$: In order to estimate the shaded background BRF, the probability P_a of a photon penetrating the canopy and then reaching the background and the collision probability P_b between a photon and foliage within canopy should be determined.

In the sunlight direction, the probability of a photon penetrating the canopy on slopes directly and then reaching the background is the gap fraction P_{ig}, which is given by GOST. If the interactions occurred $(n + 1)$ times within the canopy before this photon has reached the background, then the probability of the photon reaching the background is $(1 - Pig)\cdot w \cdot (1 - p)\cdot (p \cdot w)^n \cdot s_d$. $1 - Pig$ is the probability of a photon directly reaching the foliage, where $w = r_L(\lambda) + \tau_L(\lambda)$ is the albedo of foliage and $r_L(\lambda)$ and $\tau_L(\lambda)$ are the reflectance and transmittance of foliage, respectively. p is the probability that a photon intercepting the canopy object will recollide with other canopy elements rather than escaping the canopy space [18]. The detailed description of p can be found in the Appendix. Therefore, $1 - p$ is the probability of a photon escaping from forest canopy after collision. s_d is the downward fraction of the total scattered radiation for canopies. Therefore, the total probability of a photon penetrating the canopy and reach background is

$$P_a = Pig + (1 - Pig)\cdot w \cdot (1 - p)\cdot s_d \cdot \frac{1}{1 - p\cdot w} \tag{8}$$

where the first term is the probability of a photon reaching the background without collision and the second term is the probability of a photon reaching the background after multiple scattering. Considering multiple scattering using the p theory [19], the downward fraction of the recollision probability of a photon within the canopy is

$$\begin{aligned} P_b &= \left[w\cdot(1-p)\cdot(w\cdot p)^0 + w\cdot(1-p)\cdot(w\cdot p)^1 + \cdots \right. \\ &\qquad \left. + w\cdot(1-p)\cdot(w\cdot p)^{+\infty}\right]\cdot s_d \\ &= \frac{w\cdot(1-p)}{1-p\cdot w}\cdot s_d. \end{aligned} \tag{9}$$

The total probability of a photon penetrating the canopy (with collision), reaching the background, and finally reflecting from the background to the viewer above the canopy is $(P_a - Pig)\cdot R_G \cdot Pvg$ [Fig. 1(a)]. $P_a - Pig$ is the probability of a photon penetrating the canopy after collision. If a photon can reach the background $(n + 1)$ times [Fig. 1(b)], the probability of the photon being reflected to the view direction is $P_a \cdot R_G^2 \cdot P_b \cdot (R_G \cdot P_b)^n \cdot Pvg$. Therefore, the total probability of a photon being reflected from the background (the shaded background BRF) on a slope is

$$S_{sc}(\lambda) = R_G \cdot Pvg \cdot \left(P_a - Pig + \frac{P_a\cdot P_b \cdot R_G}{1 - P_b \cdot R_G}\right). \tag{10}$$

2) BRF of Shaded Foliage $S_{bs}(\lambda)$: For estimating the shaded foliage BRF, the upward fraction of the probability

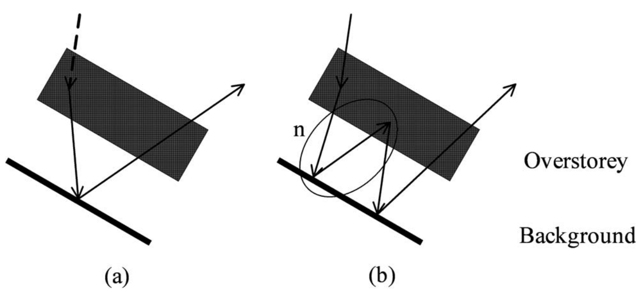

Fig. 1. Schematic of the scattering sequence of radiation reflected from background. (a) Probability of a photon penetrating the canopy from sky (with collision), reaching the background, and being reflected from the background to the viewer. The dashed line means the incident radiation interacting with foliage at least once. (b) Probability of a photon penetrating the canopy from sky (with or without collision), reaching the background ($n+1$ times, $n \geq 1$), and being reflected from the background to the viewer.

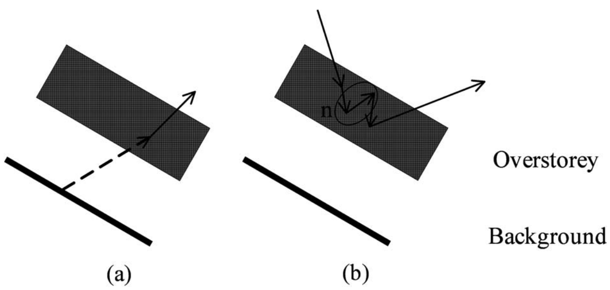

Fig. 2. Schematic of the scattering sequence of radiation reflected from foliage. (a) Probability of a photon that penetrates the canopy from the background (the dashed line means the reflected radiation interacting with foliage at least once). (b) Probability of a photon that incidents from above the canopy, being scattered within the canopy at least $n+1$ times ($n \geq 1$).

of a photon penetrating the canopy from the background P_c [Fig. 2(a)] and from the canopy itself P_d (scattered within the canopy and without considering the first-order scattering) [Fig. 2(b)] should be determined.

The upward fraction of the probability of a photon escaping from the canopy after first collision is $w \cdot (1-p) \cdot s_u$, where s_u is the upward fraction of the total scattered radiation ($s_u = 1 - s_d$). After $(n+1)$ times of collision, the upward fraction of this probability is $w \cdot (1-p) \cdot (p \cdot w)^n \cdot s_u$. Therefore, the total probability of a photon penetrating the canopy from the background P_c is

$$P_c = \frac{w \cdot (1-p)}{1 - p \cdot w} \cdot s_u. \tag{11}$$

After $(n+1)$ times of collision within the canopy, the upward fraction of the probability of a photon which reaches to the top of the sloping canopy [Fig. 2(b)] is

$$P_d = \frac{(1 - Pig) \cdot w \cdot p \cdot w \cdot (1-p)}{1 - p \cdot w} \cdot s_u. \tag{12}$$

If a photon comes from the top of the canopy and interacts with the background once, the probability of this photon escaping the canopy in the upward direction is $P_a \cdot R_G \cdot P_c$ (Fig. 3). If this photon interacts with the background $(n+1)$ times, the probability of escaping is $P_a \cdot R_G \cdot (P_b \cdot R_G)^n \cdot P_c$ (Fig. 3). Therefore, the total probability of the upward scattering from a sloping canopy after interacting with the background is $P_a \cdot R_G \cdot P_c/(1 - P_b \cdot R_G)$, while the total probability of the upward scattering from a sloping canopy is $P_a \cdot R_G \cdot P_c/(1 - P_b \cdot R_G) + P_d$.

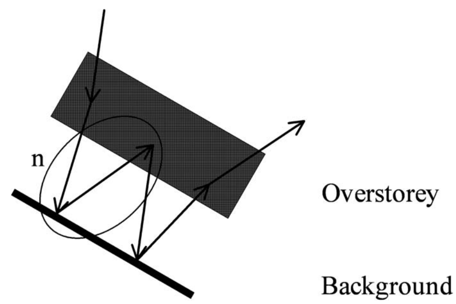

Fig. 3. Schematic of the total scattered radiation by the foliage, when the photon scattered between background and foliage $n+1$ times ($n \geq 1$).

To generate the shaded foliage BRF, a phase function is introduced as an approximation according to Omari *et al.* [4]. The phase angle is defined as $\xi^* = \cos^{-1}(\cos(\theta_s)\cos(\theta_v))$. θ_s and θ_v are the solar and view zenith angles to the sloping background. The phase function is defined as $f(\xi^*) = (1/(3\pi)(\sin\xi^* - \xi^*\cos\xi^*) + (1/3)\cos\xi^*(\tau_L(\lambda)/w(\lambda))$. Therefore, the shaded foliage BRF on sloping forests is

$$S_{bs}(\lambda) = f(\xi^*) \cdot \left(\frac{P_a \cdot R_G \cdot P_c}{1 - P_b \cdot R_G} + P_d\right). \tag{13}$$

III. Results and Discussion

A. Topographic Effects on the BRF of Shaded Components

The BRF of a sunlit component consists of the BRF due to the direct light and the BRF due to the diffuse light. Under the Lambertian assumption, the BRF of the sunlit portions does not vary with angle, although the sunlit area ratios viewed change with angle. The shaded portion is influenced by diffuse radiation in all directions and multiple sources (adjacent sunlit leaves, adjacent shaded leaves, transmission through leaves, sunlit background, and shaded background), and therefore, it is angle dependent because the contributions from these sources vary with angle. The topography of the underlying surface influences all these diffuse sources and can modify significantly the angular variation of the shaded portion of the BRF. For this reason, only the topographic effects on the shaded BRF are analyzed hereinafter.

The shaded components of BRF on sloping canopies have been theoretically simulated to show the topographic effects on the BRF of shaded components. In this paper, the following forest stand parameters are assumed: There are 4000 stems of trees per hectare with an average radius of the tree crown r of 0.85 m; the height of the lower part of the tree (trunk space) ha equals 0.5 m; the length of the crown hb equals 2.5 m; and the height of the cone equals 1.5 m.

The half apex angle α is 30°, the clumping index Ω is 0.7, and the needle-to-shoot ratio γ_E is 1.43. The solar zenith angle θ'_s and solar azimuth angle ϕs are set to 30° and 180°, and the view zenith angle θ'_v and view azimuth angle ϕv are set to 40° and 0°, respectively. The azimuth angle ϕ_g of the sloping background is set to 0° and 180°, representing the forward and backward scattering directions, respectively (Fig. 4). The mean

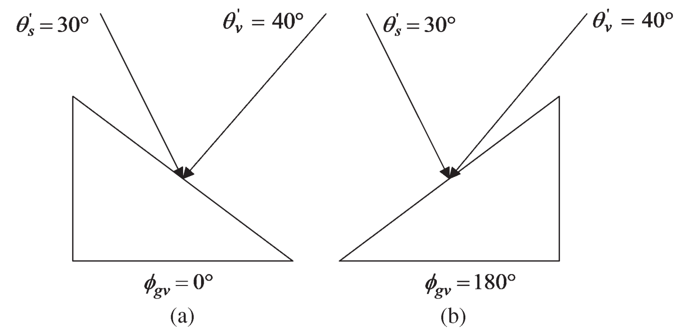

Fig. 4. Sunlight, view, and background geometry of this example shows the topographic effect on BRF of the shaded components. ϕ_{gv} is the relative azimuth angle between the viewer and the sloping background.

width of element shadows cast within tree crowns W_s equals 0.17 m. s_u and s_d are assumed to be 0.5. In the red band, the reflectance (R_T) and transmittance (τ_L) of foliage are 0.05 and 0.05, respectively; the reflectance of background (r_G) is 0.04. In the NIR band, the reflectance (R_T) and transmittance (τ_L) are 0.48 and 0.48, respectively, and the background reflectance (r_G) is 0.2.

Fig. 5 shows the topographic effects on the BRF of shaded components. According to (8), (9), and (11)–(13), $S_{bs}(\lambda)$ can be arranged as $f(\xi^*) \cdot (Pig \cdot f_1(R_G, w, p, Su, Sd) + (1-Pig) \cdot f_2(R_G, w, p, Su, Sd))$, where f_1 and f_2 are the functions of R_G, w, p, Su, and Sd. f_1 is $R_G \cdot w \cdot (1-p) \cdot Su/((1-p \cdot w) - R_G \cdot w \cdot (1-p) \cdot Sd)$, and f_2 is $R_G \cdot w \cdot (1-p) \cdot Su/((1-p \cdot w) - R_G \cdot w \cdot (1-p) \cdot Sd) \cdot w \cdot (1-p) \cdot Sd/(1-p \cdot w) + (w \cdot w \cdot p \cdot (1-p) \cdot Su/(1-p \cdot w))$. They are slightly affected by slope, but P_{ig} is strongly affected by slope. In the red band, because f_1 and f_2 are approximately equal to each other in this case, the BRF of shaded foliage is not sensitive to the topographical factors for the same leaf area index (LAI) [Fig. 5(a)]. It also shows that the BRF of shaded foliage decreases with increasing LAI due to greater radiation absorption by foliage at higher LAI.

In the NIR band, f_2 (from 0.2257 to 0.3404) is much larger than f_1 (from 0.0486 to 0.079), and therefore, the BRF of shaded foliage is determined by the quantity of incident radiation received by foliage $(1 - Pig)$. For this reason, the shaded foliage BRF on the shaded slope ($\phi_{gv} = 0°$, where ϕ_{gv} is the relative azimuth angle between the viewer and the sloping background) is higher than that on the sunlit slope ($\phi_{gv} = 180°$) due to greater radiation incident on the foliage [Fig. 5(b)]. Furthermore, the steeper a shaded slope is, the higher the shaded foliage BRF is, and the steeper a sunlit slope is, the lower the BRF of shaded foliage is.

The shaded background BRF $(Ssc(\lambda))$ is obviously influenced by topographic factors in the red and NIR bands [Fig. 5(c) and (d)]. According to (8) and (10), $Ssc(\lambda)$ can be arranged as $P_b \cdot R_G \cdot P_{vg} \cdot (P_a \cdot R_G/(1 - P_b \cdot R_G) + (1 - P_{ig}))$, where $1 - P_{ig}$ is the probability of the canopy receiving direct radiation. Therefore, $Ssc(\lambda)$ is mainly determined by the incident radiation received by the foliage in the sunlight direction and emergent radiation from the background in the view direction. $Ssc(\lambda)$ of the shaded slope ($\phi_{gv} = 0°$) is larger than that in the sunlit slope ($\phi_{gv} = 180°$). On the shaded slope, $Ssc(\lambda)$ increases with increasing slope due to foliage being exposed to more incident radiation and more radiation reflected from the shaded background in the view direction. However, on the sunlit slope, the shaded background BRF decreases with increasing slope due to foliage receiving less incident radiation while emergent radiation decreases in the view direction. Fig. 5(c) and (d) also shows that $Ssc(\lambda)$ decreases with increasing LAI in the red and NIR bands. Simply, the less incident radiation reaching the background under greater LAI conditions, the less reflected radiation is able to escape through the canopy from the background.

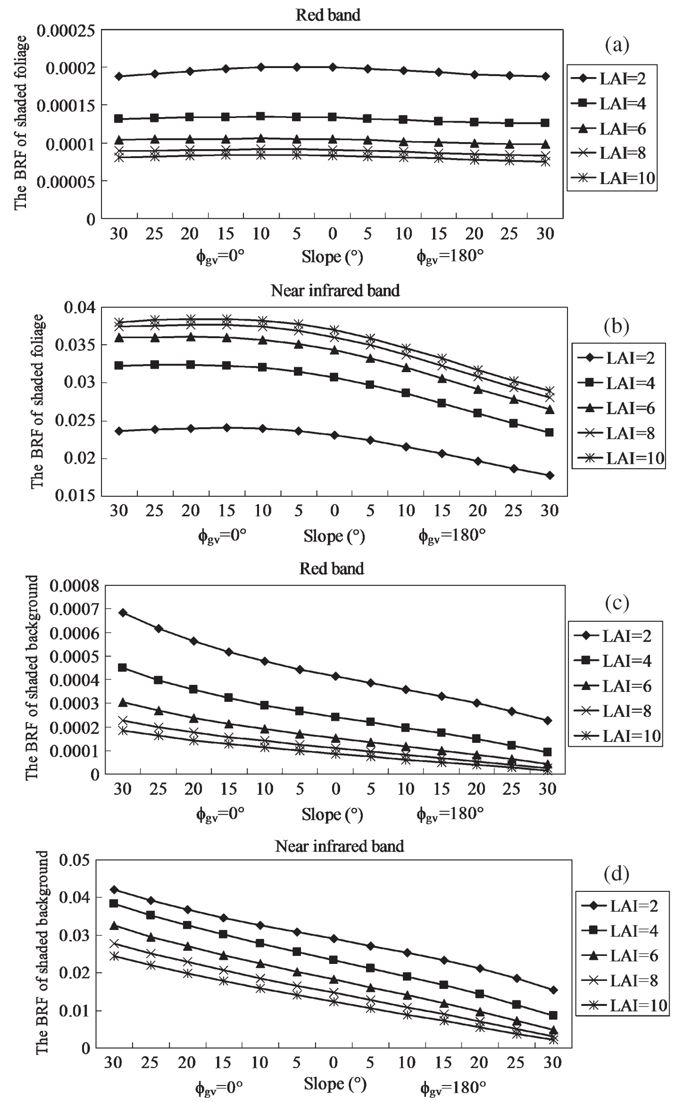

Fig. 5. Variations of BRF of the shaded components with slope and aspect in the red and NIR bands. The LAI varies from two to ten. ϕ_{gv} is the relative azimuth angle between the viewer and the sloping background.

The ratios of the shaded foliage BRF (sfBRF) to the total forest BRF (tBRF) and the shaded background BRF (sbBRF) to the total forest BRF (tBRF) are used for assessing the impact of multiple scattering on the total forest BRF under different topographic conditions (Fig. 6). Fig. 6 shows that multiple scattering on shaded slopes is larger than that on sunlit slopes for both shaded foliage and background in the red and NIR bands. The influence of multiple scattering on the total forest BRF increases with increasing slope on the shaded part of the sloping surface and decreases with increasing slope on the sunlit part.

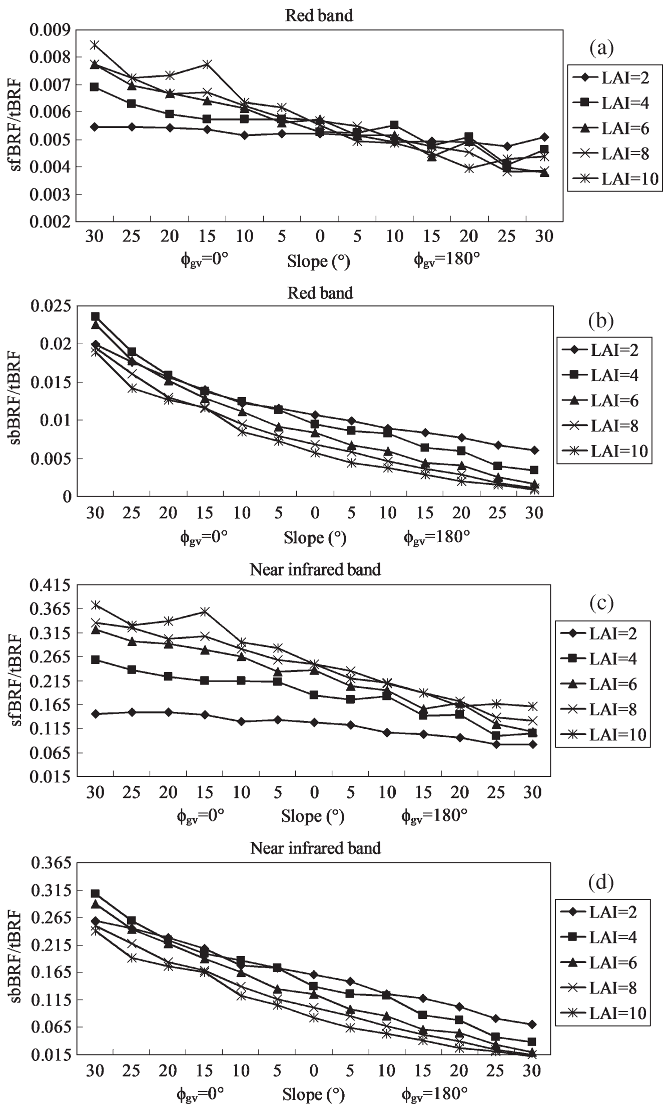

Fig. 6. Ratios between the shaded foliage BRF values and the total forest BRF values vary with slope and aspect in the red and NIR bands. LAI varies from two to ten. sfBRF/tBRF is the ratio of the shaded foliage BRF values to the total forest BRF values, and sbBRF/tBRF is the ratio of the shaded background BRF values to the total forest BRF values. ϕ_{gv} is the relative azimuth angle between the viewer and the sloping background.

In the red band, the shaded foliage BRF is only 0.3%–0.9% of the total BRF [Fig. 6(a)], and the shaded background BRF is only 0%–2.5% of the total BRF [Fig. 6(b)]. This indicates that the total BRF is captured by the first-order scattering, although the multiply scattered BRF is affected by topographical factors in the red band. According to model assumptions that first-order scattering is determined by canopy structure in the red band, the total BRF does as well. However, the shaded foliage BRF can reach up to 7%–40% of the total BRF [Fig. 6(c)], and the shaded background BRF can reach up to 1%–31% of the total BRF [Fig. 6(d)], indicating that both topographic factors and multiple scattering schemes have strong influences on the total BRF of forest on slopes. For sfBRF/tBRF [Fig. 6(a) and (c)], it can be found that the topographic influence on multiple scattering is more pronounced at greater LAI values due to increased reflection with the same level of incident radiation. For sbBRF/tBRF [Fig. 6(b) and (d)], the influence of shaded background BRF on the forest scene decreases with increasing LAI under the same topographical conditions because the probability of the photons scattered by the background escaping the canopy decreases with increasing LAI.

TABLE I
INPUT PARAMETERS OF THE NEW MODEL TO SIMULATE THE BRF OF THE THREE FORESTS

	Location 1	Location 2	Location 3
LAI	4.5	4.5	4.5
Density (trees/ha)	1440	2000	2400
Radius of crown (m)	1	1	0.5
Hb (m)	8.5	13	13
G (θ)	0.5	0.5	0.5
Ω_E	0.8	0.8	0.8
Ha (m)	6	6	6
Ws (m)	0.09	0.09	0.09
Aspect (°)	89	101	164
Slope (°)	20	18	15
R_T (red)	0.06	0.06	0.06
τ_L (red)	0.02	0.02	0.02
R_G (red)	0.15	0.15	0.15
R_T (nir)	0.5	0.55	0.55
τ_L (nir)	0.48	0.48	0.48
R_G (nir)	0.25	0.3	0.3

B. Modeled Results in Comparison With MODIS Data

Moderate Resolution Imaging Spectroradiometer (MODIS) MOD09GA reflectance data at the 500-m spatial resolution are used to validate this new model. Three sloping forest locations are selected according to slope and aspect maps generated using digital elevation models downloaded from the U.S. Geological Survey. Cloud-free reflectance values in the red and NIR bands over the course of one month at each of these three locations as well as the corresponding sunlight and view angular data with 1-km spatial resolution are collected for this validation purpose. The first study site is located at Chongqing City, China (29.6217°N/107.3798°E). Pine (*Pinus massoniana*) is the major conifer species at this study site. Eighteen cloud-free days from August 1 to 31 of 2011 are selected. The slope is 20°, and the aspect is 89° from the north. The second study site is located at Hulunbuir City, China (50.72°N/122.7309°E). Pine (*Larix gmelinii*) is the major conifer species in this study site. Seven cloud-free days from August 1 to 31 of 2011 are selected. The slope is 18°, and the aspect is 101° from the north. The third study site is located at Huma County, China (51.9989°N/123.5387°E). Pine (*Larix gmelinii*) is the major conifer species in this study site. Twelve cloud-free days from August 1 to 31 of 2011 are selected. The slope is 15°, and the aspect is 164° from the north.

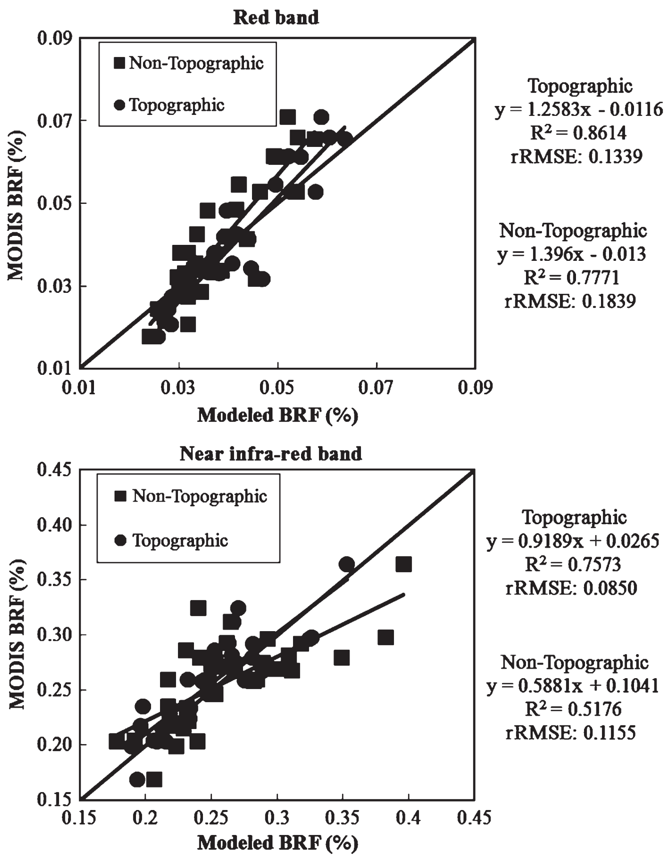

Fig. 7. Modeled BRF values with and without considering the topographic effect are compared with the MODIS BRF values on sloping terrains in the red band and NIR bands. Multiple scattering is considered in these simulations.

The input parameters of the new model for the three forests on slopes are listed in Table I. It is difficult to give observation data sets exactly for these 250 000 m^2 (500-m spatial resolution) pixels in the remote sensing images. We have made the best guess to determine the model input using common parameter values of forest within reasonable ranges. The same input parameters are used to simulate BRF using the new model with or without considering topographic factors and multiple scattering schemes. Therefore, the differences of these modeled results are not derived from these input parameters.

Fig. 7 shows the comparison of the surface reflectance (BRF product) retrieved from the MODIS image with the BRF simulated using the new method for these three sloping forest pixels. The simulated BRF of red and NIR bands which considers topographic effects compares well with the MODIS surface reflectance with R^2 values of 0.8614 and 0.7573 and rRMSE values (the ratio of the root-mean-square error to the arithmetic average of estimation result) of 0.1339 and 0.0850, respectively. If topographic effects are not considered (the slope and aspect are set as 0°), the correlations between the simulated BRF and MODIS surface reflectance values degrade considerably, with R^2 equaling 0.7771 and 0.5176 and rRMSE values of 0.1839 and 0.1155 in the red and NIR bands, respectively. Whether or not topographic factors are considered, both sfBRF/tBRF and sbBRF/tBRF are less than 1% in the red band; however, in the NIR band, sfBRF/tBRF and sbBRF/tBRF can reach up to 21% and 19% in this case, respectively. This indicates that the differences of simulated BRF between the model results with and without the topographic consideration are derived from topographic factors which are largely unaffected by the multiple scattering scheme in the red band. In the NIR band, these simulated results are not only affected by topographic factors but also affected by multiple scattering schemes. To summarize, the modeled BRF with consideration of both multiple scattering and topographic factors is closest to the MODIS surface reflectance. If the topographic factors are considered and the multiple scattering schemes are ignored, the simulated BRF values are slightly smaller than those MODIS surface reflectance values (nontopographic results in the red band), and simulated results with consideration of multiple scattering only are the worst among all simulations.

The first location is selected as an example to illustrate that the BRF of sloping forests is affected by multiple scattering in multiangle observations. Within these 18 cloud-free MODIS observations, there exist two kinds of combinations of the view azimuth angles, sunlight azimuth angles, and sunlight zenith angles. The two combinations are as follows: 1) the view azimuth angles approximately equaling 0°, the sunlight azimuth angles approximately equaling 140°, and the sunlight zenith angles approximately equaling 20° and 2) the view azimuth angles approximately equaling 97°, the sunlight azimuth angles approximately equaling 121°, and the sunlight zenith angles approximately equaling 27°. The variations of these view zenith angles are from 23° to 60° and from 1° to 62° for these two kinds of combinations, respectively. Therefore, with the consideration of the first-order and multiple scattering, the BRF values in these two planes are simulated according to these two angle combinations and compared with the MODIS surface reflectance.

Fig. 8(a) and (b) shows the comparisons between the simulated BRF and MODIS surface reflectance values for the first combination in the red and NIR bands, respectively, and Fig. 8(c) and (d) shows the comparisons between the simulated BRF and MODIS surface reflectance values for the second combination in the red and NIR bands, respectively. Similar to the preamble analysis, the BRF values are largely unaffected by multiple scattering in the red band. However, the NIR band is pronouncedly affected by multiple scattering. Generally, the simulated BRF values with consideration of multiple scattering are closer to MODIS surface reflectance. However, there are still slight differences between the simulated BRF and MODIS surface reflectance values after considering multiple scattering. This can be related to the inexact angular matching between the model and the observation, and the approximation of the complex topographical variations within the 500-m pixels with 2-D (smooth and extensive) slopes.

IV. Conclusion

In this paper, a hybrid GO–RT model for parameterizing and simulating the BRF of forests on sloping surfaces has been developed. The following conclusions can be drawn from this study.

1) LAI and topographic factors have pronounced influences on the BRF of shaded forest components. Although the

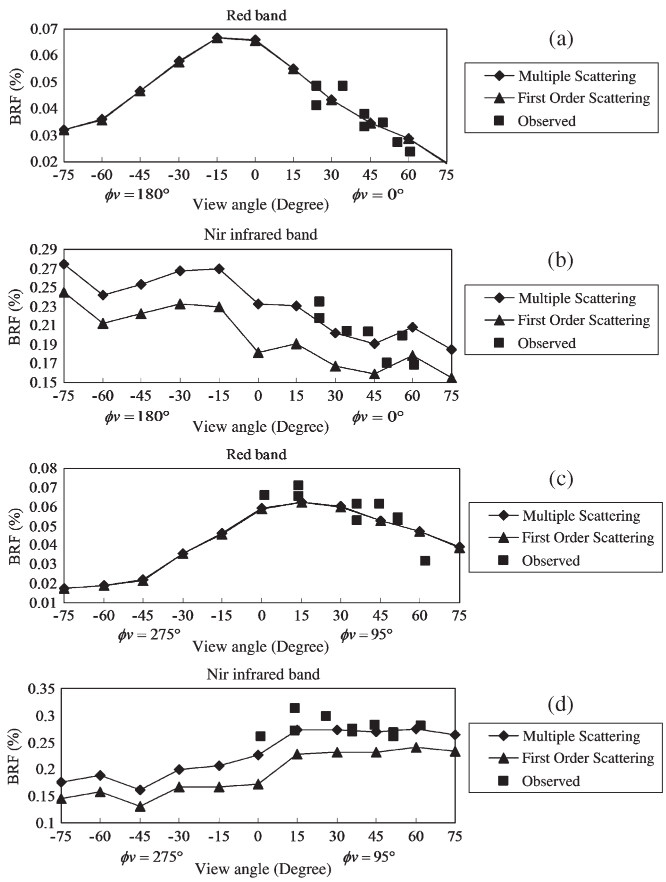

Fig. 8. Simulated BRF values compared with the MODIS BRF values at multiple angles in the red and NIR bands. The multiple scattering schemes and first-order scattering are considered in the simulated BRF, respectively.

shaded components of BRF are negligible (less than 3% of the total BRF) in the red band, the total forest BRF is strongly influenced (reaches up to 40% of the total BRF) by multiple scattering in the NIR band.

2) The new BRF model with consideration of the multiple scattering and topographic factors closely reproduced MODIS surface reflectance in three selected MODIS pixels on sloping terrains (red band: $R^2 = 0.8614$, rRMSE $= 0.1339$; NIR band: $R^2 = 0.7573$, rRMSE $= 0.0850$). If the topographic factors are considered and the multiple scattering is ignored, the simulated BRF values are slightly underestimated in the red band ($R^2 = 0.7771$ and rRMSE $= 0.1839$). Simulated results with consideration of multiple scattering and without topographic factors are worst among all simulations ($R^2 = 0.5176$ and rRMSE $= 0.1155$ in the NIR band), suggesting that the importance in considering topography is optical remote sensing.

The new model developed in this study shows the ability to simulate BRF of shaded forest components as well as the total BRF on slopes. It provides a foundation for developing a forest reflectance model for sloping forests which includes multiple scattering between neighboring sloping surfaces in complex terrains. It will also be an effective tool to improve the retrieval of the forest parameters on sloping surfaces using remotely sensed images.

APPENDIX

The parameter p is defined in previous studies as the mean recollision probability [19], [20]. They interpreted it as the probability of having two or more interactions of one photon within the canopy. The parameter p provides a useful way to model the scattering behavior of a forest canopy [4].

Smolander and Stenberg [20] indicate that the p value is practically insensitive to the solar zenith angle in the range of solar angles commonly used in satellite remote sensing, and it should be expressed for conifer (P_{CC}) and broadleaf canopies (P_{LC}), separately. For a broadleaf canopy

$$P_{LC} = P_{\max} \cdot \left[1 - e^{-k \cdot \mathrm{LAI}'^{b}}\right] \tag{14}$$

where the empirical coefficients are $P_{\max} = 0.88$, $k = 0.7$, and $b = 0.75$. For a conifer canopy

$$P_{CC} = P_{\mathrm{sh}} + (1 - P_{\mathrm{sh}}) \cdot P_{LC}(\mathrm{LAI}_m) \tag{15}$$

where $P_{LC}(\mathrm{LAI}_m)$ is the recollision probability of the broadleaf canopy with LAI equal to the modified LAI (LAI_m) for the conifer canopy. $\mathrm{LAI}_m = \mathrm{LAI}'/\gamma_E$, where γ_E is the ratio of half the total of needle area in a shoot to half the total shoot area [21]. LAI' is the LAI in the normal direction of the sloping forests. In the GOST model, LAI is defined as one-half the total leaf area per unit horizontally projected ground surface area. Therefore, $\mathrm{LAI}' = \mathrm{LAI} \cdot \cos(\theta_g)$, where θ_g is the slope of the forest background. P_{sh} is the shoot structural parameter. Smolander and Stenberg [22] indicate that the P_{sh} is closely related to $1 - 4\overline{\mathrm{STAR}}$, where $\overline{\mathrm{STAR}}$ is defined as the spherically averaged shoot silhouette to total area ratio

$$\overline{\mathrm{STAR}} = \frac{1}{\mathrm{TNA}} \cdot \frac{1}{4\pi} \int_{4\pi} \mathrm{SSA}(\Omega) d\Omega \tag{16}$$

where TNA denotes the total needle area of the shoot and $\mathrm{SSA}(\Omega)$ is the shoot silhouette area in direction Ω. Therefore, the relationship between γ_E and $\overline{\mathrm{STAR}}$ is

$$\overline{\mathrm{STAR}} = \frac{1}{4\pi \cdot \gamma_E}. \tag{17}$$

Therefore, P_{sh} can be arranged as

$$P_{\mathrm{sh}} = 1 - \frac{1}{\pi \cdot \gamma_E}. \tag{18}$$

ACKNOWLEDGMENT

The authors would like to thank Dr. T. Zheng (University of Toronto, Toronto, ON, Canada) for the helpful discussion.

REFERENCES

[1] X. W. Li and A. H. Strahler, "Geometric–optical modeling of a conifer forest canopy," *IEEE Trans. Geosci. Remote Sens.*, vol. GE-23, no. 5, pp. 705–721, Sep. 1985.

[2] J. M. Chen and S. G. Leblanc, "A 4-scale bidirectional reflection model based on canopy architecture," *IEEE Trans. Geosci. Remote Sens.*, vol. 35, no. 5, pp. 1316–1337, Sep. 1997.

[3] B. Combal, H. Isaka, and C. Trotter, "Extending a turbid medium BRDF model to allow sloping terrain with a vertical plant stand," *IEEE Trans. Geosci. Remote Sens.*, vol. 38, no. 2, pp. 798–810, Mar. 2000.

[4] K. Omari, H. P. White, and K. Staenz, "Multiple scattering within the FLAIR model incorporating the photon recollision probability approach," *IEEE Trans. Geosci. Remote Sens.*, vol. 47, no. 8, pp. 2931–2941, Aug. 2009.

[5] D. G. Gu and A. Gillespie, "Topographic normalization of Landsat TM images of forest based on subpixel sun–canopy–sensor geometry," *Remote Sens. Environ.*, vol. 64, no. 2, pp. 166–175, May 1998.

[6] V. R. Kane, A. R. Gillespie, R. McGaughey, J. A. Lutz, K. Ceder, and J. F. Franklin, "Interpretation and topographic compensation of conifer canopy self-shadowing," *Remote Sens. Environ.*, vol. 112, no. 10, pp. 3820–3832, Oct. 2008.

[7] J. Iaquinta and A. Fouilloux, "Influence of the heterogeneity and topography of vegetated land surfaces for remote sensing applications," *Int. J. Remote Sens.*, vol. 19, no. 9, pp. 1711–1723, Jun. 1998.

[8] W. L. Fan, J. M. Chen, W. M. Ju, and G. L. Zhu, "GOST: A geometric–optical model for sloping terrains," *IEEE Trans. Geosci. Remote Sens.*, vol. 52, no. 9, pp. 5469–5482, Sep. 2014.

[9] J. M. Chen and S. G. Leblanc, "Multiple-scattering scheme useful for geometric optical modeling," *IEEE Trans. Geosci. Remote Sens.*, vol. 39, no. 5, pp. 1061–1071, May 2001.

[10] M. I. Disney, P. Lewis, and P. R. J. North, "Monte Carlo ray tracing in optical canopy reflectance modelling," *Remote Sens. Rev.*, vol. 18, no. 2–4, pp. 163–196, Sep. 2000.

[11] W. Verhoef, "Light scattering by leaf layers with application to reflectance canopy modeling: The SAIL model," *Remote Sens. Environ.*, vol. 16, no. 2, pp. 125–141, Oct. 1984.

[12] S. L. Liang and A. H. Strahler, "An analytic BRDF model of canopy radiative transfer and its inversion," *IEEE Trans. Geosci. Remote Sens.*, vol. 31, no. 5, pp. 1081–1092, Sep. 1993.

[13] X. W. Li, A. H. Strahler, and C. E. Woodcock, "A hybrid geometric optical radiative transfer approach for modeling albedo and directional reflectance of discontinuous canopies," *IEEE Trans. Geosci. Remote Sens.*, vol. 33, no. 2, pp. 466–480, Mar. 1995.

[14] J. R. Miller, H. P. White, J. M. Chen, D. R. Peddle, G. McDermid, R. A. Fournier, P. Shepherd, I. Rubinstein, J. Freemantle, R. Soffer, and E. LeDrew, "Seasonal change in understory reflectance of boreal forests and influence on canopy vegetation indices," *J. Geophys. Res.*, vol. 102, no. D24, pp. 29 475–29 482, Dec. 1997.

[15] H. P. White, J. R. Miller, and J. M. Chen, "Four-scale Linear model for Anisotropic Reflectance (FLAIR) for plant canopies—Part II: Validation and inversion with CASI, POLDER, and PARABOLA data at BOREAS," *IEEE Trans. Geosci. Remote Sens.*, vol. 40, no. 5, pp. 1038–1046, May 1995.

[16] H. P. White, J. C. Deguise, J. Schwarz, J. R. Hitchcock, and K. Staenz, "Defining shaded spectra by model inversion for spectral unmixing of hyperspectral datasets—Theory and preliminary application," in *Proc. IEEE IGARSS*, 2002, pp. 989–991.

[17] A. Kuusk and T. Nilson, "A directional multispectral forest reflectance model," *Remote Sens. Environ.*, vol. 72, no. 2, pp. 244–252, May 2000.

[18] P. Lewis and M. Disney, "Spectral invariants and scattering across multiple scales from within-leaf to canopy," *Remote Sens. Environ.*, vol. 109, no. 2, pp. 196–206, Jul. 2007.

[19] Y. Knyazikhin, J. V. Martonchik, R. B. Myneni, D. J. Diner, and S. W. Running, "Synergistic algorithm for estimating vegetation canopy leaf area index and fraction of absorbed photosynthetically active radiation from MODIS and MISR data," *J. Geophys. Res.*, vol. 103, no. D24, pp. 32 257–32 276, Dec. 1998.

[20] S. Smolander and P. Stenberg, "Simple parameterizations of the radiation budget of uniform broadleaved and coniferous canopies," *Remote Sens. Environ.*, vol. 94, no. 3, pp. 355–363, Feb. 2005.

[21] J. M. Chen and J. Cihlar, "Plant canopy gap-size analysis theory for improving optical measurements of leaf-area index," *Appl. Opt.*, vol. 34, no. 27, pp. 6211–6222, Sep. 1995.

[22] S. Smolander and P. Stenberg, "A method to account for shoot scale clumping in coniferous canopy reflectance models," *Remote Sens. Environ.*, vol. 88, no. 4, pp. 363–373, Dec. 2003.

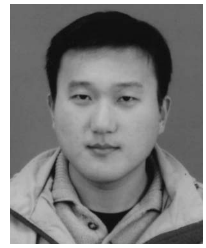

Weiliang Fan received the B.S. degree in horticulture from Shandong Agricultural University, Shandong, China, in 2007 and the M.S. degree in forest management from Zhejiang A&F University, Zhejiang, China, in 2010. He is currently working toward the Ph.D. degree at Nanjing University, Nanjing, China.

Jing M. Chen received the B.Sc. degree from the Nanjing Institute of Meteorology, Nanjing, China, in 1982 and the Ph.D. degree from Reading University, Reading, U.K., in 1986.

He is currently a Professor and the Research Chair with the Department of Geography and Program in Planning, University of Toronto, Toronto, ON, Canada. He is also an Adjunct Professor with Nanjing University, Nanjing. He has published over 200 papers in refereed journals, which have been cited over 5000 times in the scientific literature. He is currently an Associate Editor of the *Journal of Geophysical Research—Atmosphere*, the *Canadian Journal of Remote Sensing*, and the *Journal of Applied Remote Sensing*. His major research interest is in remote sensing of vegetation and quantifying terrestrial carbon and water fluxes.

Prof. Chen is a Fellow of the Royal Society of Canada.

Weimin Ju received the B.Sc. degree from the Nanjing Institute of Meteorology, Nanjing, China, in 1984 and the M.Sc. and Ph.D. degrees from the Department of Geography and Program in Planning, University of Toronto, Toronto, ON, Canada, in 2002 and 2006, respectively.

He is currently a Professor with the International Institute for Earth System Sciences, Nanjing University, Nanjing. He has published over 80 papers in refereed journals, including 45 papers in international journals. His major research interests include retrieval of vegetation parameters from remote sensing data and simulating terrestrial carbon and water fluxes.

Nadine Nesbitt is currently working toward the M.Sc. degree in the Department of Geography and Program in Planning, University of Toronto, Toronto, ON, Canada.